

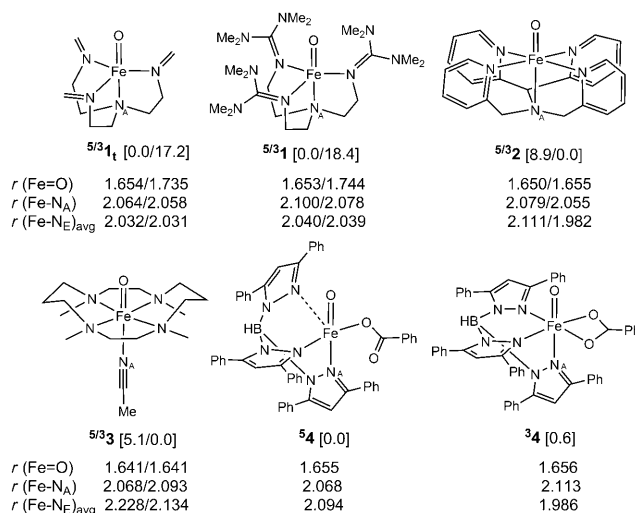
# The Fundamental Role of Exchange-Enhanced Reactivity in C–H Activation by $S = 2$ Oxo Iron(IV) Complexes\*\*

Deepa Janardanan, Yong Wang, Patric Schyman, Lawrence Que, Jr.,\* and Sason Shaik\*

Dedicated to Professor Joan Silverstone Valentine

Nonheme iron chemistry has led to the identification of a variety of iron(IV) oxo intermediates, which perform oxidative processes such as H-abstraction and oxo transfer reactions to a variety of molecules.<sup>[1,2]</sup> The advent of both enzymatic and synthetic examples has revealed a fundamental dichotomy. Whereas the known enzymatic species, for example, in taurine/ $\alpha$ -ketoglutarate dioxygenase (TauD),<sup>[3]</sup> utilize iron(IV) oxo intermediates with a quintet spin ( $S = 2$ ) ground state, the great majority of the synthetic iron oxo species have triplet ground states ( $S = 1$ ) and low-lying quintet states.<sup>[2a,c]</sup> DFT calculations suggest that the synthetic reagents should react by two-state reactivity (TSR),<sup>[4]</sup> whereby the excited  $S = 2$  state, which has a small barrier, cuts through the larger triplet-state barrier and mediates the H-abstraction process.<sup>[4,5]</sup> Given this enhanced  $S = 2$  reactivity, there is an intense search for ways to design new iron oxo reagents that have quintet ground states and that may therefore be potent C–H bond activators, like the natural enzymes.

One of us<sup>[6]</sup> recently prepared two such  $S = 2$  reagents and compared their H-abstraction activities to those of the synthetic complexes that possess the more common  $S = 1$  ground state. These results, however, generated a bag full of surprises, which are addressed herein by means of DFT calculations. Shown in Scheme 1 are the iron(IV) oxo complexes analyzed by DFT along with their key geometric features and spin-state information. The isolated complex with an  $S = 2$  ground state is  $[\text{tmg}_3\text{trenFe}^{\text{IV}}\text{O}]^{2+}$  (**1**),<sup>[6a]</sup> which possesses a trigonal bipyramidal iron coordination, typified by a two-below-two-below-one d-orbital block,<sup>[3b]</sup> and hence a



**Scheme 1.** Complexes **1–4** with key optimized bond lengths in Å (B3LYP/B1 (solvent)). Values in square brackets are  $S = 2/S = 1$  relative energies (B2) in kcal mol<sup>-1</sup>. B1 and B2 are specified in the text.  $\text{N}_E$  refers to the equatorial ligands.

quintet ground state well below the  $S = 1$  state. Surprisingly, however, **1** exhibited rather sluggish H-abstraction reactivity even towards the weak C–H bonds of 1,4-cyclohexadiene (CHD). Thus, **1** was slightly less reactive than  $[\text{N4PyFe}^{\text{IV}}\text{O}]^{2+}$  (**2**) and five times more reactive than  $[\text{tmc}(\text{an})\text{Fe}^{\text{IV}}\text{O}]^{2+}$  (**3**),<sup>[6b]</sup> both of which are thought to react by TSR.<sup>[4]</sup> To add to the puzzle, the putative  $[\text{Tp}(\text{OBz})\text{Fe}^{\text{IV}}\text{O}]$  (**4**), which was proposed to form upon oxygenation of  $[\text{Tp}(\text{benzoylformate})\text{Fe}^{\text{II}}]$  as a model for TauD, was found to be highly reactive and capable of activating even the strong C–H bond of cyclopentane (bond dissociation energy  $\text{BDE} = 96.3 \text{ kcal mol}^{-1}$ ).<sup>[6b]</sup> Note that in the  $S = 2$  state ( $^5\mathbf{4}$ ), Fe loses one of the benzoate arms and becomes a pentacoordinated square pyramid with a basal  $\text{Fe}^{\text{IV}}$  oxo moiety (Scheme 1). Thus, it is this weaker ligand field that stabilizes the  $S = 2$  state relative to the hexacoordinated  $S = 1$  state. Indeed, **4** is computed to involve degenerate  $S = 1$  and  $S = 2$  states (Scheme 1).<sup>[7]</sup> So, in **4**, a competition between the two spin states is expected to effect C–H activation; which state dominates? The experimental relative reactivities of the four  $\text{Fe}=\text{O}$  reagents order in a puzzling sequence:  $\mathbf{4} \gg \mathbf{2} \geq \mathbf{1} > \mathbf{3}$ . What is the origin of this reactivity pattern, and what are the electronic and steric factors that shape this trend? Answering this question is important for establishing rules of design of effective catalysts for C–H activation.

[\*] Dr. D. Janardanan, Dr. Y. Wang, Dr. P. Schyman, Prof. Dr. S. Shaik  
Department of Organic Chemistry and The Lise Meitner-Minerva  
Center for Computational Quantum Chemistry  
The Hebrew University, Jerusalem, 91904 (Israel)  
Fax: (+972) 2-658-4680  
E-mail: sason@yfaat.ch.huji.ac.il

Prof. Dr. L. Que, Jr.

Department of Chemistry and Center for Metals in Biocatalysis  
University of Minnesota, Minneapolis, MN 55455 (USA)  
Fax: (+1) 612-624-7029  
E-mail: larryque@umn.edu

[\*\*] We thank the National Institutes of Health (GM-33162 to L.Q.) and the Israel Science Foundation (53/09 to S.S.). P.S. thanks the Wenner-Gren Foundation for a fellowship. Dedicated to Professor Joan Silverstone Valentine in celebration of receiving the Alfred Bader Award in Bioinorganic Chemistry.

Supporting information for this article is available on the WWW under <http://dx.doi.org/10.1002/anie.201000004>.

To answer these questions, we studied the reactivities of **1–4** towards H-abstraction from CHD. The geometries of all the critical species along the H-abstraction paths of **1–3**, which are doubly positively charged, were optimized at the B3LYP/B1(CH<sub>3</sub>CN) level (B1 is LACVP) at the reaction solvent to minimize self-interaction errors that cause artificial electron transfer in some of these systems.<sup>[8]</sup> For **4**, which is neutral and hence less subject to these particular errors,<sup>[8]</sup> we used B3LYP/B1. All energies were subsequently estimated using a larger basis set, B2 (B2 is LACV3P+\*), and solvent corrections, using the solvent parameters for CH<sub>3</sub>CN for **1–3** and benzene for **4**. The details (structures, energies, and spin densities) are given in the Supporting Information.

Figure 1 shows the types of energy profiles unraveled by the calculations, where the reactant clusters (<sup>3,5</sup>RC) and <sup>3,5</sup>I are genuine minima and <sup>3,5</sup>TS<sub>H</sub> genuine transition states. Table 1 collects the barrier and reaction energy data. All calculated barriers are relative to the lowest RC (Figure 1), and hence the free energies do not include the effect of loss of entropy from association (estimated experimentally to be −18 eu for strong complexation<sup>[9]</sup>), which will increase all free energy barriers by a value of 4.4 kcal mol<sup>−1</sup> at *T* = 243 K.<sup>[9]</sup> For comparison, we show the experimental Δ*G*<sup>‡</sup> value for H-abstraction from taurine by the iron(IV) oxo species of TauD, with the *S* = 2 ground state.<sup>[3c]</sup> Since the C–H bond of taurine has a larger BDE than those of CHD (by ca. 23 kcal mol<sup>−1</sup>, Table S8 in the Supporting Information), a much lower barrier might be expected for CHD. Indeed, DFT calcu-

tions<sup>[5a]</sup> for abstraction of the allylic C–H bond in propene by iron(IV) oxo species of TauD gave a barrier of only 5.4 kcal mol<sup>−1</sup>.

Inspection of the table reveals a few trends. Firstly, the triplet-state barriers are larger than the barriers for the quintet state. In all cases, the quintet is also the ground state of the H-abstraction intermediate (<sup>3</sup>I, Figure 1). Secondly, because of the large spin-state energy gap, it is clear that **1** will react exclusively via the *S* = 2 ground state. The Δ*G*<sup>‡</sup> value for **1** seems close to the experimental value,<sup>[6a]</sup> but it does not include the entropic effect of association.<sup>[9]</sup> Regarding **4**, it is seen that, despite the degeneracy of the triplet and quintet states of the iron oxo reagent itself, its observed high reactivity<sup>[6b]</sup> must be ascribed to its reaction through the *S* = 2 state, which has a much smaller barrier than the competing *S* = 1 state. The much higher reactivity observed experimentally for **4** compared to **1**<sup>[6]</sup> is also nicely reproduced by the calculations.

Comparison of **2** and **3** reveals that the barriers on both *S* = 1 and *S* = 2 states are lower for **2**, which is in accord with experimental observation. Furthermore, the *S* = 2 barriers are gauged relative to the *S* = 1 reactant cluster species. But in fact, the *S* = 2 surface for **2** is barrier-free, whereas for **3** there is a barrier of 4–7 kcal mol<sup>−1</sup> on the different energy scales. Complexes **2** and **3** were postulated to react by TSR, with crossover from the *S* = 1 to the *S* = 2 state.<sup>[4c]</sup> Thus, if we assume that **2** and **3** react via the *S* = 2 state with a spin crossover probability close to unity, both reagents would then be predicted to be highly reactive by a few orders of magnitude more than **1**. This conclusion is, of course, in discord with the experimental data.<sup>[6a]</sup> As such, we may conclude that **2** and **3** activate CHD by a TSR scenario in which the reactions start on the *S* = 1 surface and then cross over to *S* = 2, but with a weak probability<sup>[4c,10]</sup> that lowers the rate constant to the value observed experimentally.<sup>[6a]</sup> Adding the contribution of 4.4 kcal mol<sup>−1</sup> from the loss of entropy<sup>[9]</sup> to the *S* = 2 free energy barriers in the formation of <sup>3</sup>RC, such probabilities can be roughly estimated as less than or equal to 10<sup>−3</sup>, in accord with previous estimates.<sup>[4c]</sup>

The computed high barrier and the experimentally observed<sup>[6a]</sup> sluggish reactivity of the *S* = 2 state of **1** versus the very low barriers on the *S* = 2 surfaces of all other reagents may seem odd. In the first place, we might ask: Is there a

fundamental reason why the *S* = 2 state should have such small barriers? Figure 2 shows schematic orbital occupancy changes<sup>[4b]</sup> upon going from the reactant clusters (<sup>3,5</sup>RC) to the intermediate after H-abstraction (<sup>3,5</sup>I). It is seen that the triplet process involves a shift of a β electron to a π\* d orbital of the iron oxo reagent, while a CHD radical in the φ<sub>C</sub> orbital is formed. By contrast, during the quintet reaction an α electron shifts to the σ\*<sub>z2</sub> d orbital.<sup>[4a,b]</sup> As such, in the triplet reaction the number of the stabilizing d–d exchange interac-

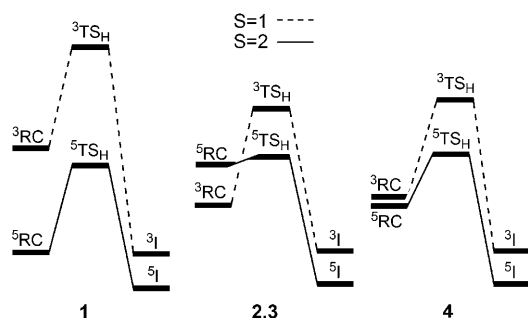


**Figure 1.** Energy profiles for the H-abstraction reactions of **1–4** with CHD. RC is the reactant cluster.

**Table 1:** Computed barriers and reaction energies (kcal mol<sup>−1</sup>) for H-abstraction reactions from CHD (C<sub>6</sub>H<sub>8</sub>) by [LFe<sup>IV</sup>O]<sup>2+</sup> reagents.

L <sup>[a]</sup>	Δ <i>E</i> <sup>‡</sup> /Δ <i>E</i> <sup>‡</sup> + ZPE/Δ <i>G</i> <sup>‡[a]</sup>		Δ <i>G</i> <sup>‡</sup> <sub>ex</sub> <sup>[e]</sup>	Δ <i>G</i> <sub>rxn</sub> <sup>[f]</sup> <i>S</i> = 1/ <i>S</i> = 2
	<i>S</i> = 1	<i>S</i> = 2		
tmg <sub>3</sub> tren ( <b>1</b> )	30.9/26.7/31.3	14.9/11.5/15.6	14.0	−3.1/−12.3
<b>1</b> <sub>t</sub> <sup>[b]</sup>		3.5 <sup>[c]</sup> /−/−	—	
N4Py ( <b>2</b> )	12.9/10.0/13.0	10.8/5.4/6.5	14.0	−15.5/−17.9
tmc(an) ( <b>3</b> )	20.3/16.6/18.8	12.0/6.2/7.1	16.1	−8.1/−15.9
Tp(OBz) ( <b>4</b> )	15.1/12.3/16.5	7.7/5.4/6.3	—	−16.1/−32.8
TauD		−5.4 <sup>[d]</sup> /−	14.8	

[a] **1–3** were optimized with solvent included. Barrier data (B3LYP/B2 with solvent corrections) are relative to the ground state of the reactant cluster (Scheme 1). [b] Truncated **1** (see text). [c] Δ*E*<sup>‡</sup> value. [d] ZPE-corrected barrier for an allylic C–H bond.<sup>[5a]</sup> [e] Calculated with the Eyring equation using rate constants for **1–3** from Ref. [6a] and for TauD from Ref. [3c]. [f] The energies of the *S* = 1/*S* = 2 intermediates relative to the lowest reactant cluster.

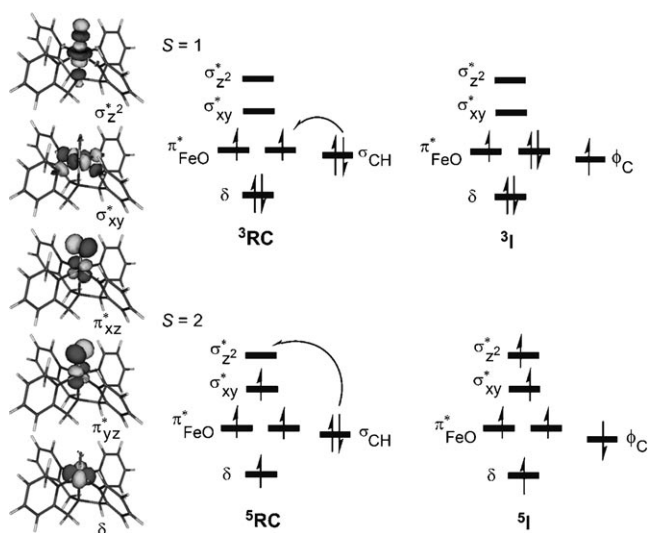


**Figure 2.** Orbital occupancy change during H-abstraction on the  $S=1$  and  $S=2$  states of an  $[LFe^{IV}O]^{2+}$  reagent (the drawn orbitals are specific to **2**). The  $^3/5I$  occupancies are related to the respective  $^3/5TS_H$ .

tions on the metal center is diminished in  $^3TS_H$ . By contrast, in  $^5TS_H$  the d–d exchange is augmented relative to  $^5RC$  by four new interactions. Thus,  $^5TS_H$  is strongly stabilized compared to  $^5RC$  by exchange interactions that lower the electron–electron repulsions. This differential stabilization in turn flattens the  $S=2$  energy profile. Furthermore, as  $^3TS_H$  is not stabilized by exchange,  $^5TS_H$  becomes the lowest-energy species<sup>[4d]</sup> in the transition-state region, even for **2** and **3**, where the  $S=2$  state starts as an excited state. The spin states thus interchange in energy in the TS region, owing to the different behavior of the corresponding exchange interactions. Hence, in general, the barrier on the  $S=1$  state is high, while that on the  $S=2$  surface is low owing to exchange-enhanced reactivity.<sup>[4a,b,5]</sup>

The orbital occupancy evolution diagram (Figure 2) also defines structural selection rules for the transition states. The TS will assume the structure that optimizes the orbital overlap between the  $\sigma_{CH}$  and the corresponding accepting orbital ( $\pi^*$  or  $\sigma^*_{z^2}$ ). The structural information for  $^5/3TS_H$  in Figure 3 indeed illustrates these selection rules, as do the trends in the barrier data in Table 1. Thus, the elongated Fe–N<sub>A</sub> bonds and the Fe–O–H angles of approximately 180° in  $^5TS_H$  reflect the occupancy of the  $\sigma^*_{z^2}$  orbital<sup>[4,11]</sup> during the  $S=2$  process, while the short Fe–N<sub>A</sub> bonds and the small Fe–O–H angles in  $^3TS_H$  are in accord with the proposed occupancy of the  $\pi^*$  orbital during the  $S=1$  process. Additionally, the O···C···H moieties of **1–4** in Figure 3 show that  $^5TS_H$  is earlier than the corresponding  $^3TS_H$  in terms of C–H bond breaking and O–H bond making, in accord with the relative barriers on the two spin surfaces. As such, the exchange-enhanced reactivity of the  $S=2$  state versus the low reactivity of the  $S=1$  state is a fundamental trend that will be true irrespective of computational accuracy.

The remaining question then is: Why is **1**, which initially has a quintet ground state, such a sluggish C–H activator? It

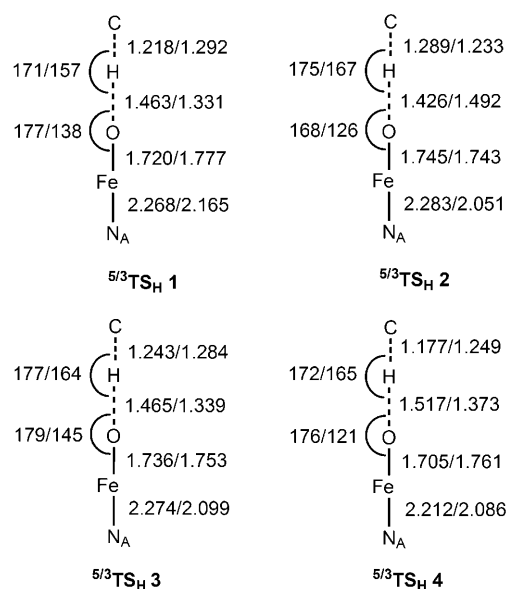


**Figure 3.** Key structural features (distances in Å, angles in degrees) in the N<sub>A</sub>–Fe–O···H···C moiety of  $^5TS_H/{}^3TS_H$  of **1–4**.

was postulated<sup>[6a]</sup> that this reactivity was due to steric effects imparted by the tetramethylguanidino substituents of the tmg<sub>3</sub>tren ligand. To test this hypothesis, we eliminated these substituents in **1**, and indeed, the  $S=2$  barrier for the H-abstraction reaction by **1** is lowered dramatically to 3.5 kcal mol<sup>−1</sup> (Table 1). Thus, the aforementioned exchange-enhanced reactivity is nicely manifested in  $^5I$ . In fact, the sluggish reactivity of **3** compared with **2** is also due to poorer access to the Fe=O moiety in **3** (Figure S8 in the Supporting Information).<sup>[11a]</sup> Clearly, a quintet ground state by itself is not sufficient to impart high reactivity to the iron(IV) oxo reagent if steric fences prohibit substrate access.

The reagent **4** seems to be an ideal solution for creating mimetic reagents of the enzymatic iron oxo species. Its benzoate ligand (see Scheme 1) provides an in situ mechanism for generating a low-lying  $S=2$  state by release of one of its arms from the iron coordination sphere, similar to the formation of the iron oxo species of TauD.<sup>[3]</sup> The Fe<sup>IV</sup>O moiety of **4** is further protected by the 3,5-phenyl substituents on two pyrazole ligands, but in a manner that creates a cleft<sup>[6b]</sup> that admits substrates selectively without imposing a great deal of steric hindrance. These properties make **4** a very potent C–H activator with shape selectivity.<sup>[6b]</sup>

In conclusion, the heightened reactivity of the  $S=2$  state of iron(IV) oxo reagents towards C–H bond activation originates in exchange-enhanced reactivity, wherein the increased number of d–d exchange interactions (Figure 2) upon going from the reactant cluster to the transition state flattens the  $S=2$  energy profile and lowers its barrier. The  $S=2$  barriers measured from the corresponding reactant cluster  $^5RC$  (Figure 1) are extremely small, for example 3.5 and 6.3 kcal mol<sup>−1</sup> for **1** and **4**, respectively, and even zero in **2**. Only steric effects can raise these barriers, as found in **1**. The nonheme enzymes, such as TauD, apparently evolved to have iron(IV) oxo reagents with an  $S=2$  ground state in order to

optimize the C–H bond activation of strong C–H bonds such as those in taurine by virtue of exchange enhancement.

Received: January 1, 2010

Published online: March 31, 2010

**Keywords:** bioinorganic chemistry · density functional calculations · iron · metalloenzymes · oxido ligands

- [1] C. Krebs, D. Galonic'-Fujimori, C. T. Walsh, J. M. Bollinger, Jr., *Acc. Chem. Res.* **2007**, *40*, 484.
- [2] a) L. Que, Jr., *Acc. Chem. Res.* **2007**, *40*, 493; b) W. Nam, *Acc. Chem. Res.* **2007**, *40*, 522; c) X. Shan, L. Que, Jr., *J. Inorg. Biochem.* **2006**, *100*, 421.
- [3] a) J. C. Price, E. W. Barr, B. Tirupati, J. M. Bollinger, Jr., C. Krebs, *Biochemistry* **2003**, *42*, 7497; b) S. Sinnecker, N. Svensen, E. W. Barr, S. Ye, J. M. Bollinger, Jr., F. Neese, C. Krebs, *J. Am. Chem. Soc.* **2007**, *129*, 6168; c) J. C. Price, E. W. Barr, T. E. Glass, C. Krebs, J. M. Bollinger, Jr., *J. Am. Chem. Soc.* **2003**, *125*, 13008.
- [4] a) D. Kumar, H. Hirao, L. Que, Jr., S. Shaik, *J. Am. Chem. Soc.* **2005**, *127*, 8026; b) H. Hirao, D. Kumar, L. Que, Jr., S. Shaik, *J. Am. Chem. Soc.* **2006**, *128*, 8590; c) H. Hirao, L. Que, Jr., W. Nam, S. Shaik, *Chem. Eur. J.* **2008**, *14*, 1740. d) As shown in Ref. [4a], a  $^5\text{TS}_\text{H}$  species generated by the shift of a  $\beta$  electron to a  $\pi^*$  orbital is  $8.2 \text{ kcal mol}^{-1}$  higher in energy than the one obtained by the  $\alpha$  electron shift to  $\sigma^*_{z^2}$  in Figure 2.
- [5] a) S. P. de Visser, *J. Am. Chem. Soc.* **2006**, *128*, 9813; b) A. J. Johansson, M. R. Blomberg, P. E. M. Siegbahn, *J. Phys. Chem. C* **2007**, *111*, 12397; c) L. Bernasconi, M. J. Louwerse, E. J. Baerends, *Eur. J. Inorg. Chem.* **2007**, 3023.
- [6] a) J. England, M. Martinho, E. R. Farquhar, J. R. Frisch, E. L. Bominaar, E. Münck, L. Que, Jr., *Angew. Chem.* **2009**, *121*, 3676; *Angew. Chem. Int. Ed.* **2009**, *48*, 3622; b) A. Mukherjee, M. Martinho, E. L. Bominaar, E. Münck, L. Que, Jr., *Angew. Chem.* **2009**, *121*, 1812; *Angew. Chem. Int. Ed.* **2009**, *48*, 1780.
- [7] For similar results on the truncated reagent, see: T. Borowski, A. Bassan, P. E. M. Siegbahn, *Inorg. Chem.* **2004**, *43*, 3277.
- [8] A. J. Johansson, M. R. Blomberg, P. E. M. Siegbahn, *J. Chem. Phys.* **2008**, *129*, 154301.
- [9] C. D. Ritchie, *Physical Organic Chemistry: The Fundamental Concepts*, Marcel Dekker, NY, **1990**. See p. 132 on experimental values for standard entropy of association.
- [10] Spin-orbit coupling, which enables the crossover from  $S = 1$  to  $S = 2$ , can be very small owing to orbital delocalization, changes in the electronic structures of the two states, and differences by more than one spin flip. See a) D. Danovich, S. Shaik, *J. Am. Chem. Soc.* **1997**, *119*, 1773; b) Y. Dede, X. Zhang, M. Schlagen, H. Schwarz, M.-H. Baik, *J. Am. Chem. Soc.* **2009**, *131*, 12634.
- [11] For analysis of electronic structures and the role of the  $\sigma^*_{z^2}$  and  $\pi^*$  d orbitals, see: a) A. Decker, J.-U. Rhode, E. J. Klinker, S. D. Wong, L. Que Jr., E. I. Solomon, *J. Am. Chem. Soc.* **2007**, *129*, 15983; b) L. Bernasconi, E. J. Baerends, *Eur. J. Inorg. Chem.* **2008**, 1672. c) For an interesting detailed orbital analysis: S. Ye, F. Neese, *Curr. Opin. Chem. Biol.* **2009**, *13*, 89.